IEEE Access
Multidisciplinary | Rapid Review | Open Access Journal

Received March 25, 2021, accepted May 18, 2021, date of publication May 21, 2021, date of current version June 1, 2021.

Digital Object Identifier 10.1109/ACCESS.2021.3082847

Analysis of Non-Idealities in the Generation of Reconfigurable Sinc-Shaped Optical Nyquist Pulses

SOUVARAJ DE[1,2], (Student Member, IEEE), ARIJIT MISRA[1], (Graduate Student Member, IEEE), RANJAN DAS[1], (Member, IEEE), THOMAS KLEINE-OSTMANN[2], AND THOMAS SCHNEIDER[1]

[1]THz-Photonics Group, Technische Universität Braunschweig, 38106 Braunschweig, Germany
[2]Department High Frequency and Electromagnetic Fields, Physikalisch-Technische Bundesanstalt (PTB), 38116 Braunschweig, Germany

Corresponding author: Ranjan Das (ranjan.das@ieee.org)

This work was supported in part by the Deutsche Forschungsgemeinschaft (DFG), German Research Foundation, under Grant 424608109, Grant 424608271, Grant 424607946, Grant 424608191, Grant 403154102, and Grant 322402243; in part by the German Research Foundation (DFG) through the Meteracom Project, Silicon-on-Insulator Basierte Integrierte Optische Frequenzkamme für Mikrowellen, THz, und Optische Anwendungen; in part by the PONyDAC Project; and in part by the Open Access Publication Funds of the Technische Universität Braunschweig.

ABSTRACT Optical sinc-shaped Nyquist pulses are widely used in microwave photonics, optical signal processing, and optical telecommunications due to their numerous advantages, like rectangular shape in the frequency domain, the orthogonality and the consequential possibility to use these pulses to transmit data with the maximum possible symbol rate. Ideal sinc pulses with the rectangular spectrum are just a mathematical construct. However, high-quality sinc pulse sequences offer the same advantages and can be generated by a phase-locked rectangular frequency comb with mode-locked lasers, intensity modulators, and integrated devices. Nevertheless, any non-idealities in the pulse and comb generation might lead to a degradation of the system performance, especially for metrology. Here, we investigate and analyze the effect of three major non-idealities, namely, the roll-off factor, the side band suppression ratio (SSR), and the ripple of sinc-shaped reconfigurable optical Nyquist pulse sequences based on 3, 5, and 9-line optical phase-locked frequency combs. We compare these results with the existing literature for the three-line comb followed by the experimental verification of the simulation results. We illustrate that by increasing the number of comb lines, the pulse sequences have superior performance and contribute to lesser root-mean-square (r.m.s.) error. We also discuss the trade-off between the r.m.s. error and the optical power loss for increasing the SSR.

INDEX TERMS Nyquist pulse, optical frequency combs, ripple, side band suppression, optical sampling.

I. INTRODUCTION

The surge in the worldwide demand for high data rate transmission to drive modern technologies and innumerable applications such as the internet of things (IoT), high-speed global networking, etc., might be attainable by optical signal processing as it provides a larger bandwidth, relatively simpler implementation and more flexibility as compared to the electrical domain. In the time domain, optical sinc-shaped Nyquist pulses [1]–[9], for instance, meet the Nyquist criterion of zero inter-symbol interference (ISI), enabling error-free transmission of overlapping pulses while encoding the data with minimum spectral bandwidth and being more tolerant of channel non-linearities and fiber dispersion [2]. Thus, they are a potential solution for data transmission with the highest possible symbol rate and for all-optical signal processing.

Until now, various methods have been reported to generate Nyquist pulses. Electronic arbitrary waveform generators (AWGs) can be used to perform Nyquist filtering of the baseband signal as illustrated in [5] and [6]. Although it provides a decent roll-off factor, the sampling rate and the processor speed are limited by the bandwidth of the electronics, and the resolution of the analog-to-digital

The associate editor coordinating the review of this manuscript and approving it for publication was Joewono Widjaja.

convertors determines the quality of the Nyquist pulses obtained.

By optical Nyquist pulse generation, higher bandwidths and roll-off factors can be obtained compared to electrical pulse shaping [10], [11]. The optical generation of Nyquist pulses was demonstrated using pulse shaping [3], mode-locked lasers, a Nyquist laser [4], and a liquid crystal spatial modulator [3], [7], for instance. In [8] and [9], optical parametric amplification and phase modulation was exploited to generate Nyquist pulses. All of these methods are generating optical pulse trains or pulse sequences. In the frequency domain, these sequences are represented by a rectangular frequency comb.

The generation of high-quality Nyquist pulse sequences based on the direct synthesis of a phase-locked, rectangular frequency comb generated by a sinusoidal modulation of cascaded Mach-Zehnder modulators (MZM) was first shown in [1]. Owing to the advantages of easy implementation, near-ideal rectangular spectrum, higher roll-off factor, and tunable repetition rate, numerous designs have been proposed based on this basic idea [12]–[17]. Lately, CMOS-compatible designs of integrated Nyquist pulse sources were in the research focus [14], [15], [13], and [18].

Besides communications, the temporal and spectral features of the pulse sequences like multi-wavelength operation and tunable repetition rate make them suitable to be used as a sampling source in photonic analog-to-digital (ADC) and digital-to-analog conversion (DAC) [15]–[17], [19]–[21] and as sampling pulses for the demultiplexing of Nyquist optical time-division multiplexing (OTDM) signals [22].

However, the effect of the non-idealities in sinc pulse sequence generation, especially for integrated solutions, has not been investigated in detail yet. This is useful for the metrological evaluation of optical sampling for THz communications, as envisaged in the research project *Metrology for THz Communications* (Meteracom) [23]. Meteracom aims at determining performance parameters of sampling techniques with a known measurement uncertainty to allow for quantitative comparisons. The non-idealities of the sinc-pulse sequences used for sampling have a direct influence on the metrological applications.

In this article, we investigate these main non-idealities for sinc-shaped Nyquist pulse sequences consisting of 3, 5, and 9 frequency lines. We will demonstrate: (i) a detailed analysis of the roll-off factor variation, optical sideband suppression, the comb ripple, and r.m.s. error, (ii) an analysis of Nyquist bandwidth on a 3-line comb for discrete roll-off scenarios with some typical modulation schemes, and (iii) finally, establishing a trade-off between the optical power and SSR for 3, 5, and 9-line combs.

The article is organized as follows: Section II analyses the non-idealities, including the roll-off factor, optical sideband suppression, and comb ripple for a 3, 5, and 9-line comb with an r.m.s. error analysis for each case. Additionally, the effect of Nyquist bandwidth due to different roll-off factors is also illustrated for several modulation schemes. Section III discusses the trade-off between optical power and SSR, followed by a conclusion and outlook in Section IV.

II. ANALYSIS OF NON-IDEALITIES

An ideal rectangular spectrum corresponds to a time-unlimited sinc-shaped Nyquist pulse, which is practically impossible to generate. However, a phase-locked and flat frequency comb with equidistant frequency components can be represented by a train of sinc pulses. As shown mathematically [1], an unlimited sinc pulse sequence is the inter-symbol interference-free superposition of equal ideal sinc pulses. Pulse sequences can be generated by filtering the frequency comb of a mode-locked laser [3], [7], by a Nyquist laser [4], by the generation of frequency combs with parametric effects [8], [9], or by one or two coupled intensity modulators that are driven with one or multiple radio frequencies [1], [12]–[21]. Especially the last method offers the possibility for integrated Nyquist pulse sources [14], [15], [13], and [18].

Assuming that there are two coupled intensity modulators, where the first modulator is driven with p and the second one with q frequencies, phase-locked to each other, the final phase-locked [1], [12], [21], and flat optical frequency comb consists of $N = (2p + 1)(2q + 1)$ equally spaced optical frequencies with a bandwidth of $B = N\Delta f$ and Δf as the separation between the subsequent frequency lines. For cascaded MZMs, the resultant combs are phase-locked, provided the RF frequencies driving those MZMs are locked in phase in the RF domain. The full-width at half-maximum (FWHM) duration of the corresponding sinc-shaped Nyquist pulse sequence is expressed as $\text{FWHM} = 0.89/(N\Delta f)$. The pulse repetition period is given as $T_s = 1/\Delta f$, and the pulse duration (from the maximum to the first zero crossings) is represented as $\tau_z = 1/(N\Delta f)$, as shown in Fig. 1. Thus, by adjusting the number of frequency comb lines N and frequency spacing Δf, the repetition rate and the pulse duration can be changed accordingly. Therefore, it is possible to reconfigure the optical Nyquist pulses according to the given requirements. Also, by appropriately tuning the phase of the electrical signal driving the modulators, the sinc pulse sequences can be shifted in time.

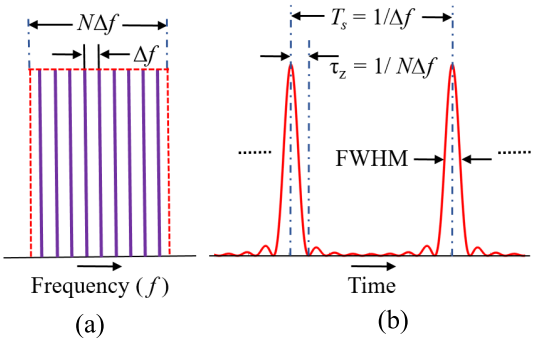

FIGURE 1. Schematic representation of an *N*-line: (a) rectangular frequency comb with linearly locked phases and, (b) the corresponding time-domain pulse sequence with the defined parameters.

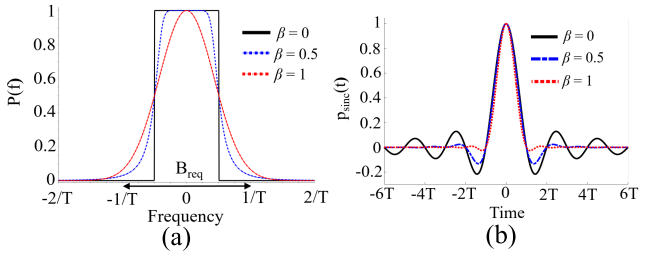

FIGURE 2. Sinc-shaped Nyquist pulses for $\beta = 0$, 0.5 and 1 in (a) the frequency and (b) the time domain. The required bandwidth (B_{req}) is given by (2).

To investigate the non-idealities in sinc pulse sequence generation, simulations are performed in Lumerical [24]. For the 3-line frequency comb with a 5 GHz spacing, these simulations are compared with experimental results. For the 5- and 9-line OFCs, the assumed frequency spacing between the comb lines Δf is 50 GHz. When single or coupled modulators generate such sequences, the minimum required bandwidth is 100 GHz for the 5-line and 150 GHz for the 9-line comb. Plasmonic modulators with bandwidths of up to 500 GHz have been demonstrated earlier [25]. However, such modulators are not available commercially, and thus we present the simulation results for 5 and 9-lines frequency comb with a 50 GHz spacing.

The following sub-sections will provide a detailed discussion and analyzes the effect of three prime non-idealities, i.e., roll-off factor (β), sideband suppression ratio (SSR), and comb ripple (R_p).

A. EFFECT OF ROLL-OFF FACTOR (β)

Generation of the Nyquist pulse sequences by optical fiber parametric amplification [8], [9] or by coupled modulators [1], [12]–[21] results in the production of several higher-order sidebands. When such sequences are generated by an MLL as provided in [3], [7], a rectangular optical filter with a very sharp out-of-band rejection is required. Since ideal rectangular filters do not exist, these filtered pulses have a roll-off factor which represents the excess bandwidth of the pulse as compared to the ideal sinc pulse ($\beta = 0$). Thus, in the frequency domain, several higher-order sidebands might be present as well.

With the defined parameters and β as the roll-off factor, the single sinc-shaped Nyquist pulse can be expressed in the time domain as:

$$p_{\text{sinc}}(t) = \text{sinc}\left(\frac{t}{\tau_z}\right) \cdot \frac{\cos\left(\beta\pi t/\tau_z\right)}{1 - (2\beta t/\tau_z)^2} \tag{1}$$

The effect of β on the pulse bandwidth and shape is shown in Fig 2. (a) and (b) respectively. Thus, sinc-shaped Nyquist pulses, represented by $\text{sinc}(t/\tau_z)$, reduce the bandwidth requirement to $1/\tau_z$ which is otherwise (i.e., $\beta \neq 0$) given by:

$$B_{\text{req}} = (1 + \beta)/\tau_z \tag{2}$$

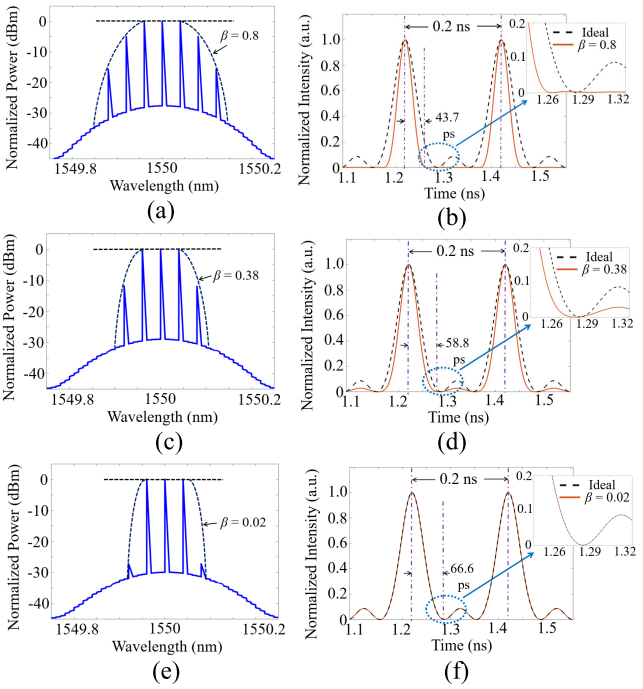

FIGURE 3. 3-line OFCs (left) with corresponding sinc-shaped Nyquist pulses (right) for $\beta = 0.8$ (a, b), $\beta = 0.38$ (c, d) and $\beta = 0.02$ (e, f). In the time domain, the ideal sinc-shaped Nyquist pulses with $\beta \sim 0$ are represented in black (dotted line) and the simulated pulses with respective roll-off are shown in orange.

To simulate the effect of the roll-off factor, a Gaussian filter with different orders is considered. The roll-off factor of zero corresponds to the ideal scenario with sinc-shaped Nyquist pulses in the time domain and a rectangular frequency comb. As shown in Fig. 3, as β increases from 0 to 1, the corresponding pulses become narrower and deviate further from the ideal shape with a reduction in the zero-crossing duration and FWHM. This occurs because with increasing β values, the filter has wider bandwidths, and hence more unwanted higher-order sidebands are included. Therefore, the total number of comb lines increases, which deteriorates the outline of the sinc-shaped Nyquist pulses.

The roll-off factor analysis is implemented for a 5- and 9-line comb with a frequency spacing of 50 GHz, as such high frequencies are used in millimeter-wave signal communication as illustrated in Fig. 4 and 5, respectively. The r.m.s. error (E_{rms}) is computed for different β values for the 3, 5, and 9-line combs using the following expression:

$$E_{\text{rms}} = \sqrt{\frac{1}{K}\sum_{i}^{K}(|p_i^m| - |p_i^I|)^2} \tag{3}$$

Here, p^m represents the measured value of the normalized intensity, and p^I represents the normalized intensity of the ideal sinc-shaped Nyquist pulse (for the i^{th} sample point). The measurement is done over a single pulse repetition period from one peak to another, considering K (total number of samples) = 10000 evaluation points. Note that the r.m.s. error (E_{rms}) for all cases in Fig. 6 reveals a comparatively lower

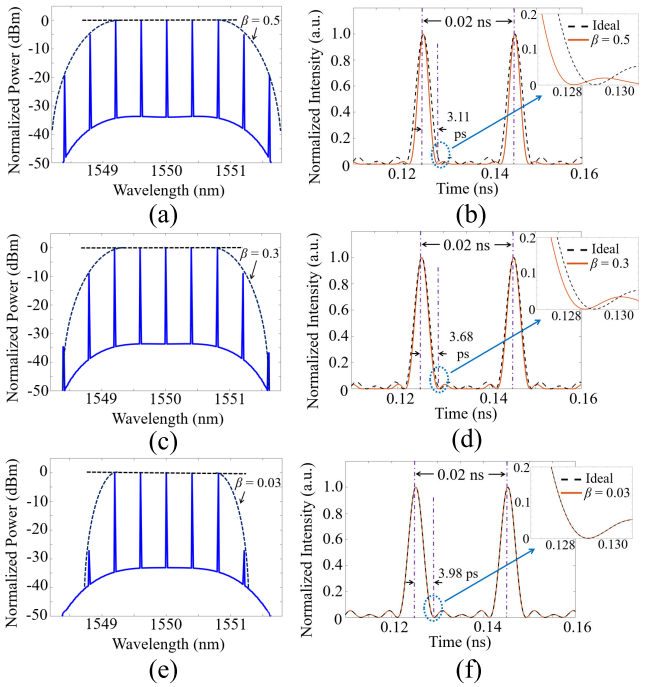

FIGURE 4. A 5-line OFC with different $\beta = 0.5$ (a, b), $\beta = 0.3$ (c, d) and $\beta = 0.03$ (e, f). Again the ideal sinc-shaped Nyquist pulse with $\beta \sim 0$ is represented in black and the simulated pulse with respective roll-off is shown in orange.

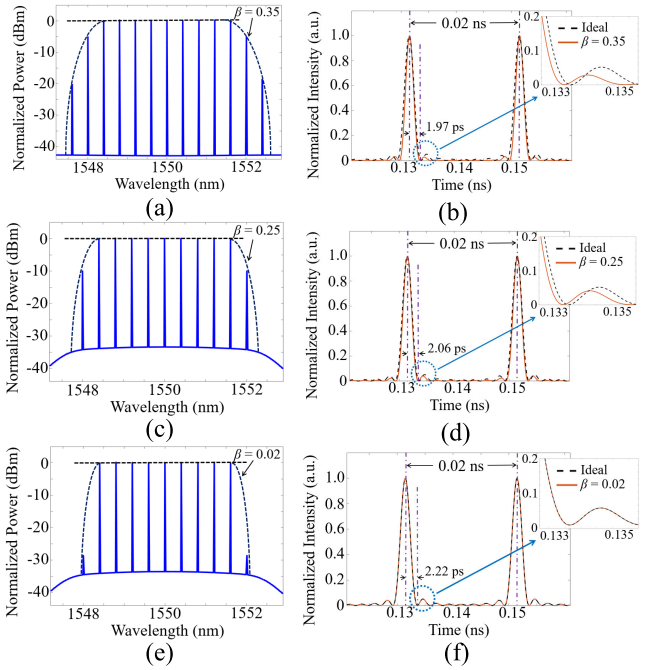

FIGURE 5. A 9-line frequency comb with several $\beta = 0.35$ (a, b), $\beta = 0.25$ (c, d) and $\beta = 0.02$ (e, f). Spectrums and pulses are shown in left and right side respectively.

error for a 9-line comb for a higher β value. Contrary to the theoretical analysis, the simulated E_{rms} starts at a slightly higher value than zero value, since zero would require an unlimited duration of the sinc pulse sequence, which is not possible for the simulation. For an r.m.s. error of below 1%

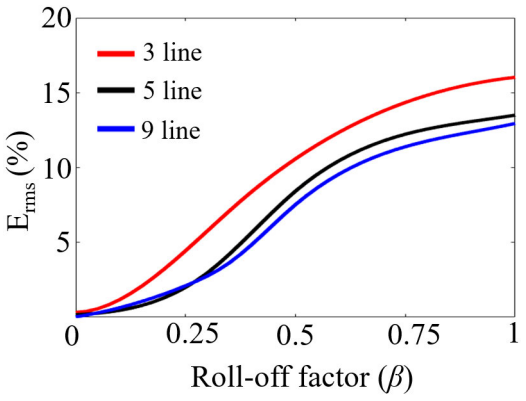

FIGURE 6. Comparison of the estimated r.m.s. errors (in %) for the 3, 5, and 9-line optical frequency combs for different roll-off factors (β).

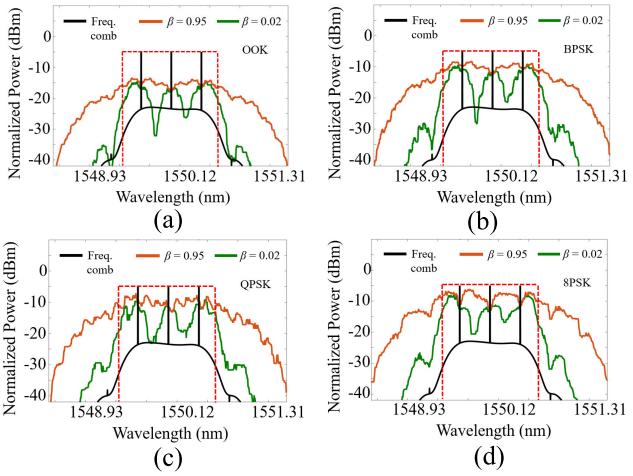

FIGURE 7. Spectrum for different roll-off factors (β) with different modulation formats, the red dotted box represents the Nyquist bandwidth.

for the 3-line comb, a roll-off factor of below 0.1 is required, whereas for the 5 and 9-line comb, a roll-off of below 0.2 is sufficient. In [26], a very sharp rectangular filter with a roll-off of 0.02 has been achieved by fiber based Brillouin losses. However, conventional optical filters like the WaveShaper 1000A by Finisar report a best possible β of around 0.10. If the 9-line comb is directly generated by two coupled modulators, the sideband suppression is around 30 dB [1]. This can be compared with a filtered comb with a roll-off factor of 0.02, which is difficult to achieve by optical filtering.

B. EFFECT OF THE ROLL-OFF FACTOR ON MODULATIONS

The effect of the Nyquist bandwidth for modulated sinc pulse sequences is investigated for a 3-line OFC with the frequency spacing (Δf) = 50 GHz and a corresponding bandwidth of 150 GHz with two extreme β values (i.e., 0.02 and 0.95) for some typical modulation schemes, namely, OOK, BPSK, QPSK, and 8-PSK respectively, as shown in Fig. 7. Note that in each of these cases, a higher β value increases the effective bandwidth due to the inclusion of undesired higher-order sidebands in the frequency spectrum. However, for a low β, as achievable with coupled modulators, the signal spectrums

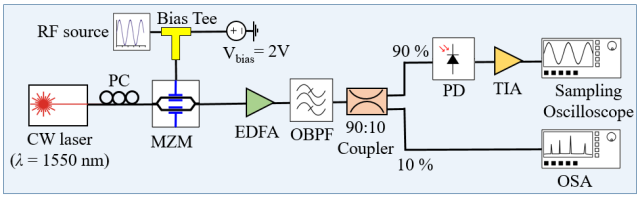

FIGURE 8. Experimental setup for a comb generation with 3 lines. The additional RF source for the higher-order sideband generation is not shown here.

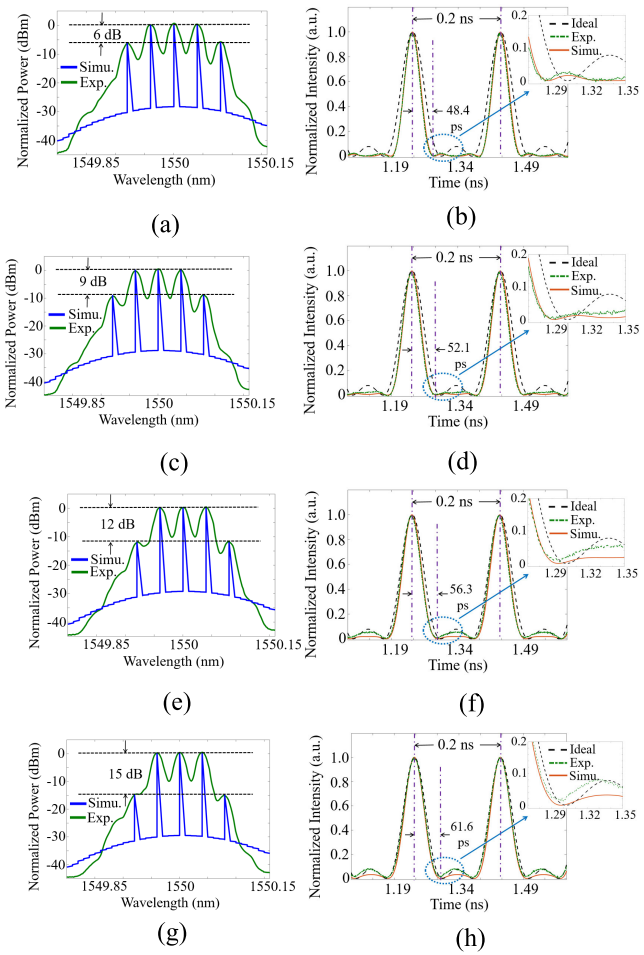

FIGURE 9. 3-line OFCs with corresponding sinc-shaped Nyquist pulses for 6 dB SSR (a, b), 9 dB SSR (c, d), 12 dB SSR (e, f), and 15 dB SSR (g, h). In the frequency domain, the simulated frequency spectrum is shown in blue, while the experimental spectrum is shown in green. Please note that due to the restricted bandwidth of the optical spectrum analyzer, the frequency lines for the experiment appear to be much broader than they really are. In the time domain, the ideal sinc-shaped Nyquist pulse with an SSR of around 35 dB is represented in black, and the experimental and simulated pulse is shown in green and orange, respectively.

(green curves) are almost entirely confined within the Nyquist bandwidth (shown by red dotted box).

C. EFFECT OF SIDE BAND SUPPRESSION RATIO (SSR)

If the sinc pulse sequence is generated by the filtering of a frequency comb, the SSR can be controlled by changing the order of the filter as depicted in Figs. 3 - 5. Alternately,

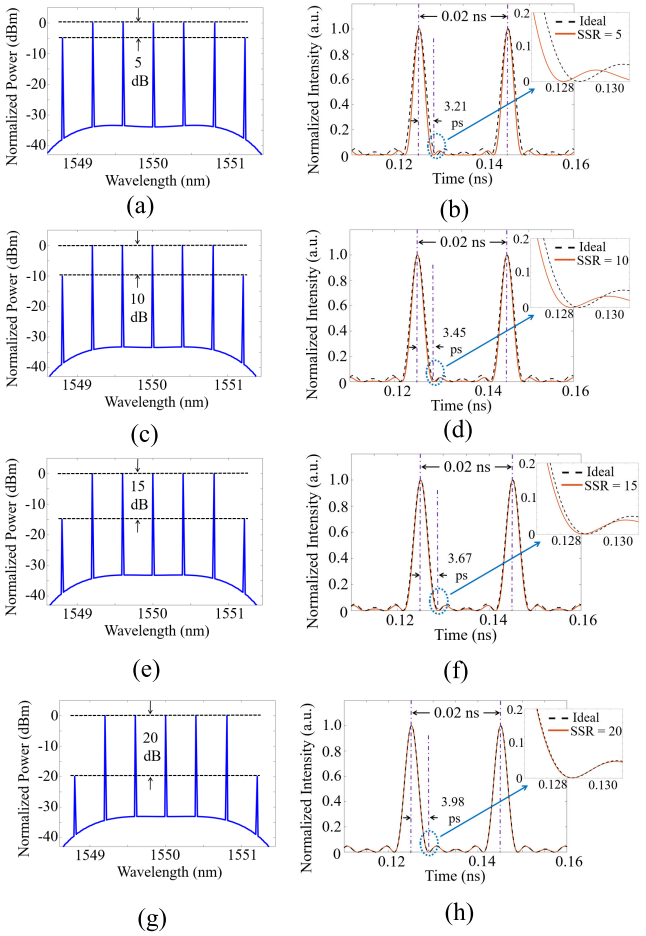

FIGURE 10. 5-line OFCs (left) with corresponding sinc-shaped Nyquist pulses (right) for 5 dB SSR (a, b), 10 dB SSR (c, d), 15 dB SSR (e, f) and 20 dB SSR (g, h). In the time domain, the ideal sinc-shaped Nyquist pulse sequence with an SSR of around 35 dB is represented in black, and the simulated pulse with respective SSR is shown in orange.

the SSR can directly be adjusted by tuning the bias voltage and the RF-power when it is generated by one or two coupled modulators [12]. Unlike the roll-off factor analysis, the simulated analysis of the SSR includes the first higher-order sideband only. To investigate the effects of the SSR experimentally, a setup as shown in the schematic diagram in Fig. 8 is used. We have used a similar method [1] to generate sinc-shaped Nyquist pulses and analyzed the non-idealities in detail which has not been thoroughly discussed yet. Such a metrological evaluation of optical pulses is essential for mm-wave or THz signal sampling as envisaged in the research project 'Meteracom' [23]. A 3-line OFC is generated by modulating a CW source at 1550 nm by a single tone RF signal with 5 GHz frequency, generated from an RF generator (ANRITSU MG3692A) with a $LiNbO_3$ based Mach-Zehnder Modulator. The input light polarization to the MZM was carefully aligned by a polarization controller (PC). A separate DC source is used to ensure the proper biasing of the MZM. The resulting signal is then amplified by an Erbium-doped fiber amplifier (EDFA) and passed

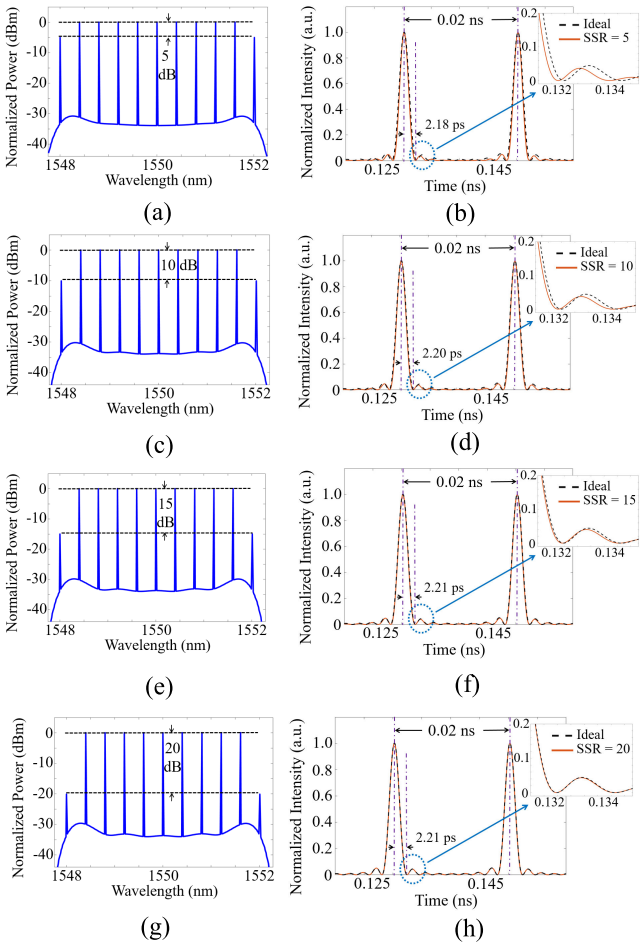

FIGURE 11. 9-line OFCs (left) with corresponding sinc-shaped Nyquist pulses (right) for 5 dB SSR (a, b), 10 dB SSR (c, d), 15 dB SSR (e, f) and 20 dB SSR (g, h). The ideal sinc-shaped Nyquist pulse with an SSR of around 35 dB and the simulated pulse sequence obtained in each scenario is shown in black and orange, respectively.

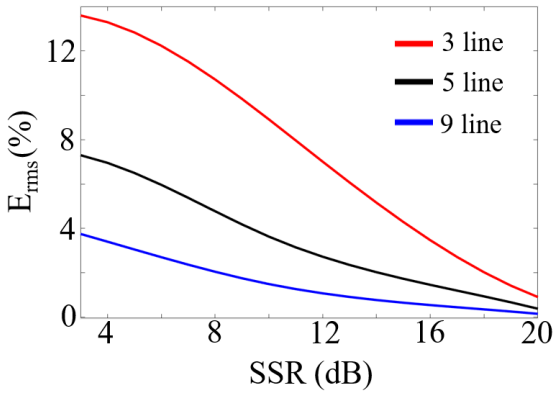

FIGURE 12. Comparison of estimated r.m.s. errors (in %) for a 3, 5 and 9-line comb for different SSR (dB).

through an optical band-pass filter with a central wavelength of 1550 nm. The filter has a bandwidth of 50 GHz and is just used to reduce the amplified spontaneous emission noise generated by the EDFA. The 90:10 fused fiber coupler splits 10% of the signal power to the optical spectrum analyzer (YOKOGAWA AQ3670C) to determine the frequency

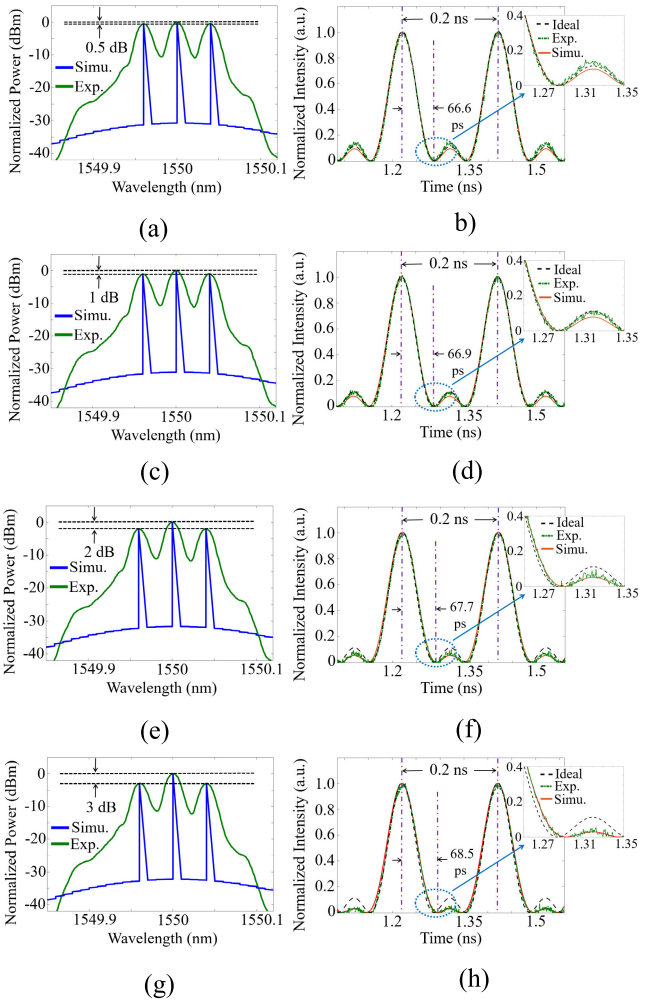

FIGURE 13. 3-line comb with corresponding sinc-shaped Nyquist pulse sequence for 0.5 dB ripple (a, b), 1 dB ripple (c, d), 2 dB ripple (e, f) and 3 dB ripple (g, h). The ideal sinc-shaped Nyquist pulse train without a ripple and an SSR of around 35 dB are represented in black, and the simulated pulses with respective ripple (R_p) are shown in orange.

spectrum. The remaining 90% power is applied to a Finisar photodiode (PD) with a bandwidth of 40 GHz connected to an electrical sampling oscilloscope (Agilent 86100C) for the visualization in the time domain. To investigate the SSR, additional sidebands are introduced at 10 GHz using another sinusoidal source that is synchronized to the primary RF source. A similar simulation setup is adopted using Lumerical [24] for comparison. Ideally, the sinc-shaped Nyquist pulses should have a periodicity of 0.2 ns, a FWHM (Full Width at half maximum) of 59.33 ps, and a pulse duration of 66.67 ps. The sideband suppression ratio (SSR), which is defined as the difference (in dB) between the peak power and the highest power in the sidebands, can be changed by fine-tuning the power from the second RF source. The corresponding outputs are examined in the frequency and time domain, as demonstrated in Fig. 9.

As can be seen from the results of the 5 GHz frequency spacing, or the pulses with 5 GHz repetition rate, respectively, raising the SSR subsequently improves the pulse

TABLE 1. Comparison of R.M.S. errors for sinc-pulse sequences.

Reference	[1]	[14]	[15]	[13]		[18]			This work		
Type of modulator	Cascaded MZMs[a]	Cascaded MZMs[a]	Si MZM[a]	$LiNbO_3$ based DP-MZM[b]		Si based DP-MZM[b]			Cascaded and single MZMs[a]		
Number of OFC lines	9	9	3	5		5			3	5[#]	9[#]
Frequency spacing (GHz)	10	5	12	10	20	5	8	10	5	50	50
Pulse duration (ps)	11.11	22.22	27.77	20	10	40	25	20	66.67	4	2.22
r.m.s. error (%)	0.98 (SSR[d] > 27 dB)	3.68 (R_p[c] = 2.92 dB)	U.A.[*]	1.10 (SSR[d] = 31.2 dB)	2.37 (SSR[d] = 28.7 dB)	3.7 (R_p[c] = 1.7 dB)	3.7 (R_p[c] = 2.1 dB)	3.8 (R_p[c] = 1.9 dB)	1.38 (SSR[d] = 20 dB)	0.52 (SSR[d] = 20 dB)	0.19 (SSR[d] = 20 dB)
									0.81 (R_p[c] = 0.5 dB)	0.66 (R_p[c] = 0.5 dB)	0.48 (R_p[c] = 0.5 dB)

MZM[a] = Mach-Zehnder modulator, DP-MZM[b] = Dual-parallel Mach-Zehnder modulator, R_p[c] = Ripple, SSR[d] = Side band suppression ratio, U.A.[*] = Unavailable, [#] = Simulation.

duration and FWHM and shows an increased congruence to the ideal pulses. Thus, as for the filter with a higher roll-off, with an increased SSR, the higher-order sideband's influence reduces, and the waveform distortion is decreased significantly. The experimental results slightly differ from the simulation results due to the non-ideal E/O response of the $LiNbO_3$ based MZM used in the experiment.

As can be seen from the zoomed view in Fig. 9(b), for a poor SSR of only 6 dB the generated sequences highly mismatch with the ideal ones. On the contrary, when the SSR increases to 15 dB as observed in Fig. 9(h), the sidelobe intensity decreases significantly, and the sequence closely follows the ideal sinc-shaped Nyquist pulses. The experimental results slightly differ from the simulated one as they have different spectrums.

Similarly, the SSR analysis for a 5- and 9-line OFC with 50 GHz frequency spacing and a repetition time of 0.02 ns is implemented by simulation. The 5-line OFCs are simulated by modulating two sinusoidal signals at 50 GHz and 100 GHz, respectively, with an MZM. The 9-line OFCs are modeled by cascading two MZMs and electrically modulating the first with a sinusoidal frequency of 50 GHz and the second with a frequency of 150 GHz, phase-locked to the first. The sinc-shaped Nyquist pulses have an FWHM of 3.56 ps and 1.97 ps and a zero-crossing duration of 4 ps and 2.22 ps for the 5-line and 9-line comb, respectively. Increasing the SSR from 5 dB to 20 dB, as shown in Fig. 10 and Fig. 11, results in an increase in the zero-crossing duration and FWHM and an increased resemblance to the ideal sinc-shaped Nyquist pulses while maintaining the same period.

The r.m.s. error (E_{rms}) is computed rigorously for different SSR values for the 3, 5, and 9-line combs, as shown in Fig. 12. It is calculated using (3) with 10000 evaluation points. An increase in the number of comb lines corresponds to a narrowed pulse width and an increased number of lobes which explains the significant reduction in the E_{rms} for lower SSR values with an increase in the number of lines.

D. OFC RIPPLE (R_p) EFFECT

Ripple in the spectrum of a sinc-pulse sequence can be observed due to finite passband ripple in an optical bandpass filter when it is generated by filtering a frequency comb. For the pulse sequence generation by modulators, the ripples can occur due to an insufficient adjustment of the bias and RF power. In the experimental setup, the combs are analyzed in the frequency and time domain for different values of ripple by adjusting the bias voltage of the MZM, as illustrated in Fig. 13. It is observed that increasing the ripple value results in a further deviation from the ideal scenario with a reduction in the zero-crossing duration (τ_z) and FWHM in the time domain while maintaining the same repetition rate. For a lower ripple value e.g., 0.5 dB as per Fig. 13(b), the main lobe of the measured and the ideal sinc-shaped Nyquist pulses coincide with each other, and there exists a slight mismatch in the side lobe, where the measured pulse has a sinc-shaped Nyquist pulse; resulting in a high inconsistency in the side lobe of the measured and the ideal pulse.

The ripple analysis is done for 5- and 9-line combs with a frequency spacing of 50 GHz as well, as shown in Fig. 14 and Fig. 15, respectively. Finally, the r.m.s. error (in %) is calculated using (3) with 10000 data points for a 3, 5, and 9-line

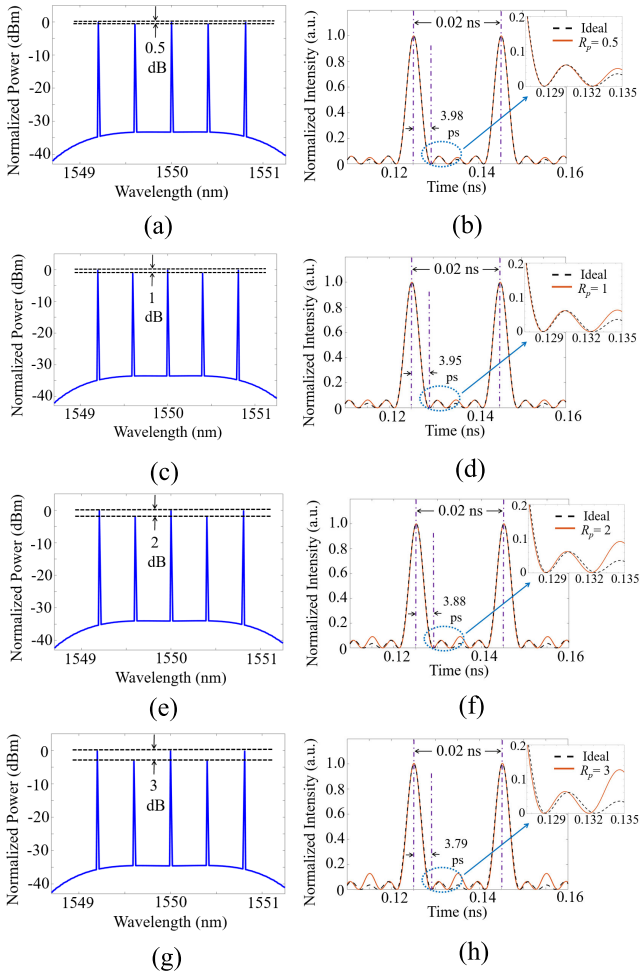

FIGURE 14. 5-line OFCs with corresponding sinc-shaped Nyquist pulses for 0.5 dB ripple (a, b), 1 dB ripple (c, d), 2 dB ripple (e, f) and 3 dB ripple (g, h). The ideal sinc-shaped Nyquist pulse with an SSR of around 35 dB and the simulated pulse obtained in each scenario in the time domain is shown in black and orange, respectively.

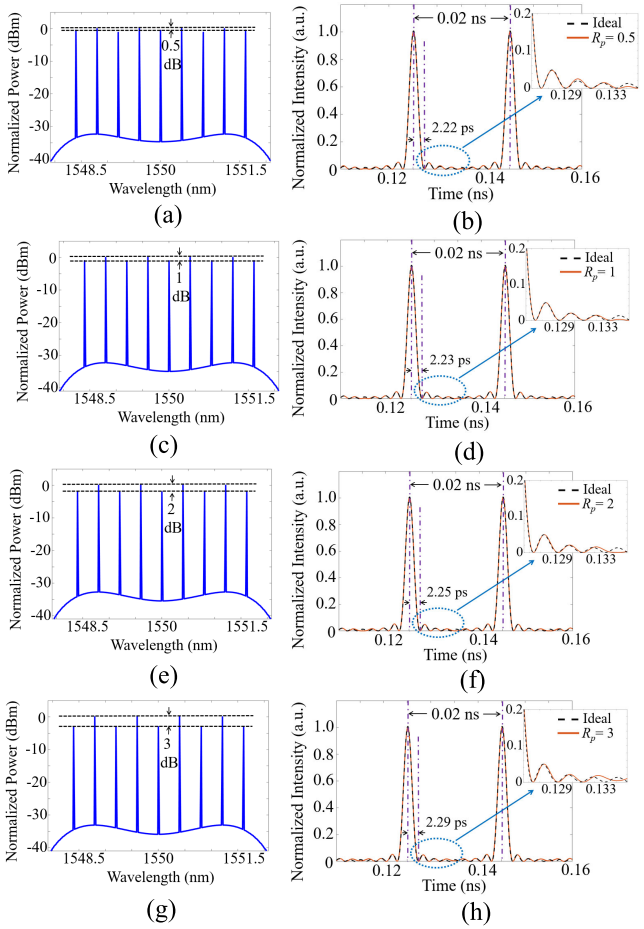

FIGURE 15. 9-line OFCs with corresponding sinc-shaped Nyquist pulses for different ripple values. Again, the ideal sinc-shaped Nyquist pulse sequence (SSR = 35 dB) and the simulated pulse with respective roll-off are shown in black and orange, respectively.

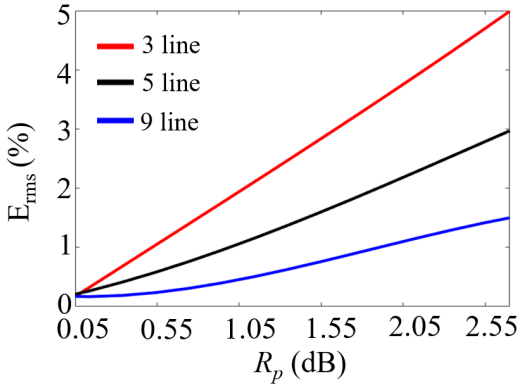

FIGURE 16. Comparison of the estimated r.m.s. errors (in %) for the 3, 5 and, 9-line comb for different ripple values (R_p).

comb as depicted in Fig. 16. It reveals a slightly better performance with lesser error for the 9-line scenario. Even for a three-line comb generation by integrated silicon modulators, a ripple of just 0.04 dB has been shown in [15]. However, the ripple might increase to 1.83 dB for coupled modulators and other integrated designs [14].

A comparison of several parameters across previously reported works involving ripple and r.m.s. error is provided in Table 1 with different types of modulators. References [1] and [13], utilizes non-integrated modulators to generate the Nyquist pulse sequences. In [1], two cascaded MZMs were used whereas [13] incorporates a single dual-parallel MZM. Reference [15] is using an electronic-photonic integrated MZM for all-optical sampling. Similarly, silicon-based integrated modulators are used in [14] and [18]. Our work provides a comprehensive analysis of the effect of non-idealities in Nyquist pulses, namely, roll-off factor, SSR and ripple including r.m.s. error for 3-line, 5-line, and 9-line combs.

To summarize the results, the error due to SSR and roll-off factor is much higher than the passband ripple in a spectrum of a sinc sequence. Thus, SSR and roll-off factor play a critical role in the accurate generation of sinc-pulse sequences and hence for optical sampling.

III. DISCUSSION

If the unwanted first-order sidebands are filtered out with a filter, a part of the optical power is lost which can be

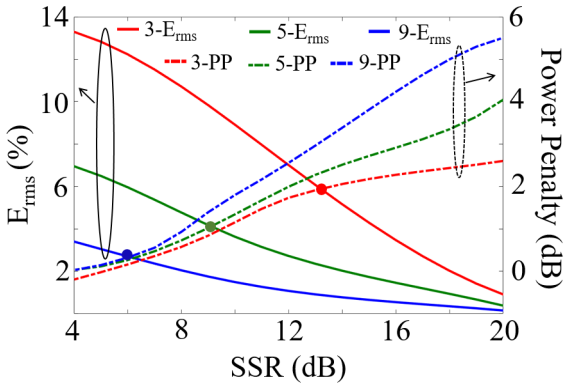

FIGURE 17. The plot of r.m.s. error and power penalty (in dB) for different values of SSR. The solid red, green and blue line represents the r.m.s. error for the 3, 5, and 9-line combs, respectively, whereas the dotted lines represent the power penalties (PP). Solid circles indicate the optimum operating point for the respective frequency comb.

considered as a power penalty while generating sinc-shaped Nyquist pulses and it is measured by monitoring optical power at the filter (optical) input and output. This power penalty has been investigated in Fig.17 for the 3, 5, and 9-line comb. The power loss increases with the SSR, leading to a reduction of the optical power of the pulse at the output. At the same time, the suppression of the sidebands decreases the r.m.s. error as explained in Sec. II C, leading to a much better shape of the pulse. Hence, for optimum performance of the system, both of these factors need to be considered, and thus, there is a trade-off between the r.m.s. error and the optical power loss. Interestingly, the 9-line comb has the highest optical power loss but the lowest r.m.s. error. A design curve like Fig. 17, which contains trade-off parameters, is useful to determine the suitable operating point for a 3, 5, or 9-line frequency comb based sinc-shaped Nyquist pulse sequence. If the maximum tolerable r.m.s. error is 5%, for instance, the required SSR for a 3-line comb would be around 15 dB and the power penalty is 2.5 dB. If a lower r.m.s. error (<5%) is desired then a 5- or 9-line comb can be considered with an optimum operating point as indicated in Fig. 17.

IV. CONCLUSION AND OUTLOOK

In this work, the effect of non-idealities for sinc-shaped Nyquist pulse generation such as roll-off factor, sideband rejection ratio (SSR), and ripple has been investigated thoroughly for a 3, 5, and 9-line comb which can further be extended for a higher frequency spacing between the comb lines. The simulation results are compared with experiments for the 3-line comb and also with previously reported results. It has been found that the 9-line combs have the lowest r.m.s. error and thus have improved performance. Also, the effect of Nyquist bandwidth due to different roll-off factors for modulated sinc-pulses has been explored for a 3-line comb, and it is verified that a lower roll-off corresponds to a much higher confinement of the information in the channel bandwidth for some popular modulation schemes. A trade-off between the r.m.s. error, or the shape and the optical power of the output pulses have been obtained for different SSRs.

In future, the experimental validation of non-idealities for 5- and 9-line combs will be performed at a frequency spacing of 50 GHz to provide a complete evaluation in the mm-wave range suitable for metrology applications. Furthermore, as a next step in the investigation of the performance of a Nyquist pulse-based sampling approach compared to conventional electrical sampling, methods from waveform metrology will be adopted. This includes the determination of the transfer function with associated measurement uncertainty in the form of a covariance matrix that takes into account the correlation between all measurement points. Furthermore, parameters such as the effective number of bits (ENOB), jitter, linearity, and effective bandwidth will be derived with measurement uncertainty to allow for a quantitative performance comparison with other sampling approaches.

ACKNOWLEDGMENT

The authors would like to thank Dr. Kai Baaske from Physikalisch-Technische Bundesanstalt (PTB) and S. Preussler, K. Singh, C. Feng, J. Kadum, Y. Mandalawi, and J. Meier from TU-Braunschweig for useful discussions on waveform metrology and measurements.

REFERENCES

[1] M. A. Soto, M. Alem, M. A. Shoaie, A. Vedadi, C.-S. Brès, L. Thévenaz, and T. Schneider, "Optical sinc-shaped Nyquist pulses of exceptional quality," *Nature Commun.*, vol. 4, no. 1, p. 2898, Dec. 2013.

[2] H. Toshihiko, R. Hirata, J. Wang, M. Yoshida, and M. Nakazawa, "Single-channel 10.2 Tbit/s (2.56 Tbaud) optical Nyquist pulse transmission over 300 km," *Opt. Exp.*, vol. 26, no. 21, pp. 27221–27236, 2018.

[3] M. Nakazawa, T. Hirooka, P. Ruan, and P. Guan, "Ultrahigh-speed 'orthogonal' TDM transmission with an optical Nyquist pulse train," *Opt. Exp.*, vol. 20, no. 2, pp. 1129–1140, Jan. 2012.

[4] M. Nakazawa, M. Yoshida, and T. Hirooka, "The Nyquist laser," *Optica*, vol. 1, no. 1, pp. 15–22, Jul. 2014.

[5] R. Schmogrow, M. Winter, M. Meyer, D. Hillerkuss, S. Wolf, B. Baeuerle, A. Ludwig, B. Nebendahl, S. Ben-Ezra, J. Meyer, M. Dreschmann, M. Huebner, J. Becker, C. Koos, W. Freude, and J. Leuthold, "Real-time Nyquist pulse generation beyond 100 Gbit/s and its relation to OFDM," *Opt. Exp.*, vol. 20, pp. 317–337, Jan. 2012.

[6] R. Schmogrow, D. Hillerkuss, S. Wolf, B. Bäuerle, M. Winter, P. Kleinow, B. Nebendahl, T. Dippon, P. C. Schindler, C. Koos, W. Freude, and J. Leuthold, "512QAM Nyquist sinc-pulse transmission at 54 Gbit/s in an optical bandwidth of 3 GHz," *Opt. Exp.*, vol. 20, no. 6, pp. 6439–6447, 2012.

[7] T. Hirooka, P. Ruan, P. Guan, and M. Nakazawa, "Highly dispersion-tolerant 160 Gbaud optical Nyquist pulse TDM transmission over 525 km," *Opt. Exp.*, vol. 20, pp. 15001–15007, Jul. 2012.

[8] A. Vedadi, M. A. Shoaie, and C.-S. Brès, "Near-Nyquist optical pulse generation with fiber optical parametric amplification," *Opt. Exp.*, vol. 20, no. 26, p. B558, 2012.

[9] M. A. Shoaie, A. Mohajerin-Ariaei, A. Vedadi, and C.-S. Brès, "Wideband generation of pulses in dual-pump optical parametric amplifier: Theory and experiment," *Opt. Exp.*, vol. 22, no. 4, pp. 4606–4619, 2014.

[10] R. Schmogrow, S. Ben-Ezra, P. C. Schindler, B. Nebendahl, C. Koos, W. Freude, and J. Leuthold, "Pulse-shaping with digital, electrical, and optical filters—A comparison," *J. Lightw. Technol.*, vol. 31, no. 15, pp. 2570–2577, Aug. 15, 2013.

[11] S. El Amari, M. Kenaan, C. Merla, B. Vergne, D. Arnaud-Cormos, P. Leveque, and V. Couderc, "Kilovolt, nanosecond, and picosecond electric pulse shaping by using optoelectronic switching," *IEEE Photon. Technol. Lett.*, vol. 22, no. 21, pp. 1577–1579, Nov. 1, 2010, doi: 10.1109/LPT.2010.2073458.

[12] M. A. Soto, M. Alem, M. A. Shoaie, A. Vedadi, C.-S. Brès, L. Thévenaz, and T. Schneider, "Generation of Nyquist sinc pulses using intensity modulators," in *Proc. CLEO*, Jun. 2013, pp. 1–2.
[13] J. Wu, J. Zang, Y. Li, D. Kong, J. Qiu, S. Zhou, J. Shi, and J. Lin, "Investigation on Nyquist pulse generation using a single dual-parallel Mach-Zehnder modulator," *Opt. Exp.*, vol. 22, no. 17, pp. 20463–20472, Jan. 2014.
[14] S. Liu, K. Wu, L. Zhou, L. Lu, B. Zhang, G. Zhou, and J. Chen, "Optical frequency comb and Nyquist pulse generation with integrated silicon modulators," *IEEE J. Sel. Topics Quantum Electron.*, vol. 26, no. 2, pp. 1–8, Mar. 2020.
[15] A. Misra, C. Kress, K. Singh, S. Preußler, J. C. Scheytt, and T. Schneider, "Integrated source-free all optical sampling with a sampling rate of up to three times the RF bandwidth of silicon photonic MZM," *Opt. Exp.*, vol. 27, no. 21, pp. 29972–29984, Oct. 2019.
[16] A. Misra, S. Preußler, L. Zhou, and T. Schneider, "Nonlinearity- and dispersion-less integrated optical time magnifier based on a high-Q SiN microring resonator," *Sci. Rep.*, vol. 9, no. 1, pp. 1–11, Dec. 2019, doi: 10.1038/s41598-019-50691-2.
[17] S. Preussler, N. Wenzel, and T. Schneider, "Flexible Nyquist pulse sequence generation with variable bandwidth and repetition rate," *IEEE Photon. J.*, vol. 6, no. 4, pp. 1–8, Aug. 2014, doi: 10.1109/JPHOT.2014.2331240.
[18] S. Liu, K. Wu, L. Zhou, L. Lu, B. Zhang, G. Zhou, and J. Chen, "Microwave pulse generation with a silicon dual-parallel modulator," *J. Lightw. Technol.*, vol. 38, no. 8, pp. 2134–2143, Apr. 15, 2020, doi: 10.1109/JLT.2020.2964102.
[19] V. Vercesi, D. Onori, J. Davies, A. Seeds, and C.-P. Liu, "Photonic sampling of broadband QAM microwave signals exploiting interleaved optical Nyquist pulses," in *Proc. Opt. Fiber Commun. Conf.*, Mar. 2018, pp. 1–3.
[20] S. Preußler, G. R. Mehrpoor, and T. Schneider, "Frequency-time coherence for all-optical sampling without optical pulse source," *Sci. Rep.*, vol. 6, no. 1, p. 34500, Dec. 2016, doi: 10.1038/srep34500.
[21] J. Meier, A. Misra, S. Preusler, and T. Schneider, "Orthogonal full-field optical sampling," *IEEE Photon. J.*, vol. 11, no. 2, pp. 1–9, Apr. 2019, doi: 10.1109/JPHOT.2019.2902726.
[22] T. Hirooka, D. Seya, K. Harako, D. Suzuki, and M. Nakazawa, "Ultrafast Nyquist OTDM demultiplexing using optical Nyquist pulse sampling in an all-optical nonlinear switch," *Opt. Exp.*, vol. 23, no. 16, pp. 20858–20866, 2015.
[23] D. Humphreys, M. Berekovic, I. Kallfass, C. Scheytt, T. Kürner, A. Jukan, T. Schneider, T. Kleine-Ostmann, M. Koch, and R. Thomä, "An overview of the meteracom project," in *Proc. 43rd Wireless World Res. Forum (WWRF)*, London, U.K., Oct. 2019.
[24] Lumerical. (Jan. 2021). *INTERCONNECT: Photonic Integrated Circuit Simulator*. [Online]. Available: https://www.lumerical.com/products/
[25] M. Burla, C. Hoessbacher, W. Heni, C. Haffner, Y. Fedoryshyn, D. Werner, T. Watanabe, H. Massler, D. L. Elder, L. R. Dalton, and J. Leuthold, "500 GHz plasmonic Mach-Zehnder modulator enabling sub-THz microwave photonics," *APL Photon.*, vol. 4, no. 5, May 2019, Art. no. 056106.
[26] C. Feng, S. Preussler, and T. Schneider, "Sharp tunable and additional noise-free optical filter based on Brillouin losses," *Photon. Res.*, vol. 6, no. 2, pp. 132–137, 2018.

SOUVARAJ DE (Student Member, IEEE) received the B.Tech. degree in electronics and communication engineering from the National Institute of Technology at Calicut, Calicut, India, in 2016, and the M.Tech. degree in optoelectronics and optical communication from IIT Delhi, India, in 2020.

He has been working as a Visiting Researcher with the THz Photonics Group, Technische Universität Braunschweig, Germany, since 2019. He is currently working as the Scientist of Physikalisch-Technische Bundesanstalt (PTB), Braunschweig, Germany. His current research interests include silicon photonics, high-frequency communication, and THz photonics for 6G and beyond. He was a recipient of the DAAD Fellowship.

ARIJIT MISRA (Graduate Student Member, IEEE) received the M.Sc. degree in physics from the Indian Institute of Engineering, Science and Technology, Howrah, India, in 2015. He was a Research Assistant with the Centre for Nano-Electro-Mechanical Systems and Nanophotonics, IIT Madras, before joining the Institute for High-Frequency Technology, TU Braunschweig, Germany, in 2017, as a Ph.D. student. His research interests include integrated photonic devices design, fabrication, and characterization, and their application to optical signal processing.

RANJAN DAS (Member, IEEE) received the B.E. degree in electronics and instrumentation engineering from Jadavpur University, India, and the master's and Ph.D. degrees from the Electrical Engineering Department, IIT Bombay, Mumbai, India, in 2018. He was a Visiting Researcher with the Electronics and Electrical Engineering Department, Southern University of Science and Technology, Shenzhen, China. He is currently a Postdoctoral Researcher with Technische Universität Braunschweig, Germany. His major research interests include THz photonics for wireless communication, photonic signal processing, integrated photonics, reconfigurable microwave components designs, and real-time analog signal processing.

THOMAS KLEINE-OSTMANN was born in Lemgo, Germany, in 1975. He received the M.Sc. degree in electrical engineering from the Virginia Polytechnic Institute and State University, Blacksburg, VA, USA, in 1999, and the Dipl.Ing. degree in radio frequency engineering and the Dr.Ing. degree from Technische Universität Braunschweig, Braunschweig, Germany, in 2001 and 2005, respectively. He was a Research Assistant with the Ultrafast Optics Group, Joint Institute of the National Institute of Standards and Technology and the University of Colorado, Boulder, CO, USA, and with the Semiconductor Group, Physikalisch-Technische Bundesanstalt (PTB), Braunschweig, before he started working on the Ph.D. degree in the field of THz spectroscopy at Technische Universität Braunschweig. Since 2006, he has been with the Electromagnetic Fields Group, PTB. He has been working on realization and transfer of the electromagnetic field strength, electromagnetic compatibility, antenna measuring techniques, and THz metrology. In 2007, he became the Head of the Electromagnetic Fields Group. In 2012, he became the Head of the Electromagnetic Fields and Antenna Measuring Techniques Group. In 2020, he became the Head of the Department of High Frequency and Fields, PTB. He is a member of the VDE and the URSI and Privatdozent at TU Braunschweig. He received the Kaiser-Friedrich Research Award, in 2003, for his work on a continuous-wave THz imaging system.

THOMAS SCHNEIDER received the Diploma degree in electrical engineering from Humboldt Universität zu Berlin, Berlin, Germany, in 1995, and the Ph.D. degree in physics from Brandenburgische Technische Universität Cottbus, Cottbus, Germany, in 2000. From 2000 to 2013, he was with the Deutsche Telekom Hochschule für Telekommunikation (HfT), Leipzig, Germany. From 2006 to 2013, he was the Head of the Institut für Hochfrequenztechnik, HfT. Since 2014, he has been the Head of the Terahertz-Photonics-Group, Institut für Hochfrequenztechnik, Technische Universität Braunschweig, Braunschweig, Germany. His current research interests include nonlinear optical effects in telecommunication systems and sensors, slow and fast light, high-resolution spectroscopy, the generation of millimeter and THz waves, optical sampling, and integrated photonics.